View Online

Demonstration of sandwich and competitive modulated supraparticle fluoroimmunoassay applied to cardiac protein biomarker myoglobin

Mark A. Hayes,*[a] Matthew M. Petkus,[a] Antonio A. Garcia,[b] Tom Taylor[c] and Prasun Mahanti[d]

Received 16th June 2008, Accepted 17th November 2008
First published as an Advance Article on the web 16th December 2008
DOI: 10.1039/b809665a

Published on 16 December 2008 on http://pubs.rsc.org | doi:10.1039/B809665A
Downloaded by Arizona State University on 06 November 2010

Modulated supraparticle structures are used to improve sandwich and competitive fluoroimmunoassays. The improved methods are demonstrated on myoglobin, a key diagnostic protein for detection of heart damage. The resulting method uses microliter volumes with bovine serum samples doped with varying concentrations of equine myoglobin. These immunoassays use micron-diameter iron oxide particles as a solid phase for antibody anchoring. Introduction of a magnetic field creates dipole moments on the particles, which attracts them to each other to form rod-like supraparticle structures. These structures can rotate within an alternating magnetic field generating convective flow and a periodic signal that can be analyzed with lock-in amplification enabling more sensitive detection. The system is demonstrated on a target associated with acute myocardial infarction (AMI). This disease causes decreased oxygen delivery to the heart resulting in tissue death and the release of cardiac myoglobin into the bloodstream. Studies have shown that the assessment and monitoring of serum myoglobin concentrations is important when making an early diagnosis of AMI. Early diagnosis is crucial since treatment is most effective when done within the first two hours of symptoms. The modulated assay is rapid, accurate, and sensitive for myoglobin assessment of small-volume serum samples. Using a cut-off value of 5.0 nM (85 ng/mL) for AMI induced myoglobin, the modulated competitive assay was able to diagnose AMI-like conditions in serum doped with myoglobin after an incubation time of only 10 min. The standard curve developed for the modulated sandwich assay was linear over a range of zero to 1 nM (17 ng/mL) with a lower limit of detection at 50 pM (0.85 ng/mL).

Introduction

The impact of analytical biochemistry on medical care will continue to grow. This growth will be driven by an increasing number of medically important biomolecular targets being identified and confirmed, then assessed across populations and within individuals.[1,2] New technologies which allow the economic and timely measurement of those biomarkers will enable the impact to be widely felt. One example where analytical biochemistry will undoubtedly have a positive impact is the care of acute myocardial infarction (AMI) patients. Infarction is a deadly short-term condition where an obstruction hinders blood flow and oxygen delivery to the heart causing tissue death. Treatment of this condition requires reperfusion therapy where either thrombolytic drugs are administered to break down the blockage, or an angioplasty is performed to expand vessel walls and induce blood flow. If reperfusion therapy is not administered in time, the heart is damaged beyond repair, as myocardial salvage decreases exponentially and falls below 50% after a two-hour period.[3,4] To ensure minimal cardiac damage, a fast and accurate diagnosis of AMI is needed, preferably within two hours. An inaccurate diagnosis not only wastes valuable medical resources on healthy individuals, but it can also result in death.

Currently, the electrocardiogram (ECG), not biomarkers, is the most commonly used AMI diagnostic. Unfortunately, ECG analysis may be subtle and open to interpretation, leading to inconsistent diagnosis, as the sensitivity for AMI is as low as 60%.[5] However, biomarkers are becoming more prominent in analysis; several have been identified as being released into the blood during an AMI event. The current consensus focuses on creatine kinase, troponins, and myoglobin.[6–8] Of the three, myoglobin is released earliest into the bloodstream, making it the best candidate marker for early diagnosis.[7,9,10]

We have chosen AMI diagnosis and the biomarker myoglobin to demonstrate the utility of our developing immunoassay technology. This technology is part of a larger strategy to fully integrate the chemical information content of biofluids by monitoring multiple biomarkers in parallel and over short time periods. The basis of this strategy is to examine the change, or slope, of concentration *versus* time, for all of the significant biomarkers. This analytical technique has the potential to convey critical information as well as provide a personal baseline of each patient. The strategies used in this work are aimed at the long-term goal.

[a]*Department of Chemistry and Biochemistry, Arizona State University, Main Campus, P.O. Box 871604, Tempe, AZ 85287-1604, USA. E-mail: MHayes@ASU.edu; Fax: +1-480-965-2747; Tel: +1-480-727-6482*
[b]*Harrington Department of Bioengineering, Arizona State University, Tempe, AZ 85287-9709, USA*
[c]*School of Mathematics, Arizona State University, Tempe, AZ 85287-1804, USA*
[d]*Department of Electrical Engineering, Arizona State University, Tempe, AZ 85287-5706, USA*

This journal is © The Royal Society of Chemistry 2009

View Online

Published on 16 December 2008 on http://pubs.rsc.org | doi:10.1039/B809665A
Downloaded by Arizona State University on 06 November 2010

In terms of diagnostics, AMI cannot be discounted if serum myoglobin is above ~5 nM (85 ng/mL). However, some AMI victims do not reach these levels until several hours after the infarction, with a peak at approximately five hours.[9] Furthermore, other AMI patients do not display serum myoglobin concentrations over a set threshold, leading to false negative diagnoses.[9–11] Studies suggest that misdiagnosis of AMI could be prevented by examining serial measurements of serum myoglobin combined with sensitivity well below 5 nM.[10–12]

There are several commercial approaches to measuring myoglobin in blood, in addition to new strategies that are still in the demonstration phase.[13–17] The most sensitive commercial assay is the two-site enzyme immunoassay marketed by Dade Behring Inc.[10,12,18,19] This immunoassay requires a laboratory-sized Stratus® CS Stat Fluorimetric Analyser. An evaluation of this system for myoglobin requires a minimum of 3.0 mL of whole blood (~1.7 mL serum) with an analysis time of 2 h.[19] The detection limit of this assay is reported as 56 pM (1 μg/L) (2 SD over zero measurement) with a linear range of 56 pM–50 nM (1.0–900 μg/L). Although this system shows good range with low detection limits, factors such as analysis time, sample volumes, and the inability to make rapid serial measurements prevents early diagnosis of AMI.[12] A related commercial system in common use is the iSTAT, which does not monitor myoglobin, but three other markers which arise later in the post-AIM response.[20–22] An immunoturbidimetric assay for myoglobin makes rapid serial measurements of myoglobin from 2.8 to 36 nM (50–650 μg/L).[11] This assay measures the dynamic changes of myoglobin over time, but fails to diagnose some AMI patients within initial hours if their concentrations fall below the detection limit. In a diagnostic test involving 126 total patients, 35% of the 51 patients having AMI were not diagnosed by the immunoturbidimetric assay. Additionally, a novel SPR sensor has been developed to monitor myoglobin *in vivo*; in buffer the detection ranges from 160 pM to 5.6 nM (2.9–100 μg/L). However, non-specific binding has limited its use in serum.[23] These types of analysis require multiple sample preparation steps to be performed to prevent non-specific binding and high background signal.[5,23–26]

Other groups are also working to improve the immunoassay of myoglobin. Le Moigne *et al.* examined the VIDAS system from bioMerieux, based on an enzyme-linked fluorescent immunoassay method, and suggested that this system had equivalent performance to other commercial systems (detection limit 5 ng/mL, dynamic range 100 ng/mL, precision <5%).[17] Newer academic approaches include a colloidal gold electrochemical system that has not yet demonstrated equivalent performance to commercial systems, although it holds some promise.[16] Other systems rely on improved luminosity from local field effects, and are also relatively unproven – yet holding promise once developed further.[13–15] Other strategies to accomplish immunoassay quickly and sensitively could be adapted to the cardiac targets, but they have yet to be applied to this problem.[27–29] A sensor with the capability to make rapid measurements within the first hour of AMI, such as the immunoturbidimetric assay but with a better detection limit, could potentially lower the mortality rate for AMI by as much as 6.5%.[4]

Several general approaches to immunoassay exist.[30] According to terminology in Wild (2005),[30] these include direct assays, where the antigen target is labeled, sandwich assays, where the antigen binds two antibodies, one of which is labeled, and lastly competitive assays, where a labeled antigen competes with the sample antigen for the binding site. We have demonstrated direct assay for small molecules[31] and here show competitive and sandwich assays for protein. This approach is focused on reducing background noise while minimizing incubation times by utilizing rotors created from paramagnetic particles to both generate convective mixing and encode the optical signal.[31] This is both an extension of the rotors-based strategy and an example application. While the details of this application are important and defended in this article, the approach of removing background noise and encoding the optical signal with the solid phase surface is a general approach and can be used in a number of applications. This modulation and deconvolution approach described in the present work can also be used in combination with other optical improvements to myoglobin immunoassays (enhanced luminosity, for example)[13–15] to leverage the capabilities and improve the overall performance of the combined systems.

Our research entails fast and sensitive immunoassays that use small volumes that can also be highly parallelized. To do this, we are using enhanced convective mixing and physical optical encoding. Both of these are accomplished by using paramagnetic particles as the solid support of the immunoassay in a colloidal solution.[32] When exposed to a magnetic field, the paramagnetic particles form dipole moments and are attracted to each other forming rod-like supraparticle structures.[33] When the magnetic field is alternated, the rod-like structures rotate with the same phase and frequency as the magnetic field. Data were collected on an inverted fluorescence microscope, where multiple 15 μL-sized droplets were analyzed for each assay solution. Using a cylindrical rare earth magnet, the magnetic field was rotated at a constant frequency, typically at 1.5 Hz. The pixel intensity average for over 100 consecutive frames from approximately two supraparticle structures (150 × 120 pixels from a total image of 348 × 260 pixels, ~20 frames/s) was captured (Fig. 1). The average pixel intensities calculated for each selection were then plotted *versus* time, and lock-in amplification calculations were performed on the normalized periodic raw signal (more details in the Experimental section and ref. 31). This gives several advantages for speed and improved detection limits. The particles are in a free colloid during the capture and wash phases, allowing for quick and efficient interrogation of the full sample volume. Formation and rotation of the rotors adds to convective flow and allows the encoding of the optical single in a discernable pattern. In addition to improving signal intensity, lock-in amplification minimizes background noise which leads to improved detection limits by over an order of magnitude.[31,34]

The current abilities of this approach are shown with equine myoglobin in bovine serum through competitive and sandwich fluoroimmunoassays. The competitive assay demonstrates a quick diagnostic test for serum myoglobin concentrations greater than or equal to a 5 nM threshold. The sandwich assay can provide for the analysis of serum samples taken in series over time to accurately quantify serum myoglobin concentrations from 50 pM to 1 nM. Better detection limits and dynamic range are expected from image and signal processing beyond the lock-in strategy[35] and more refined experimental protocols. Specifically, we recognize that we do not effectively exploit the

 This journal is © The Royal Society of Chemistry 2009

View Online

Published on 16 December 2008 on http://pubs.rsc.org | doi:10.1039/B809665A
Downloaded by Arizona State University on 06 November 2010

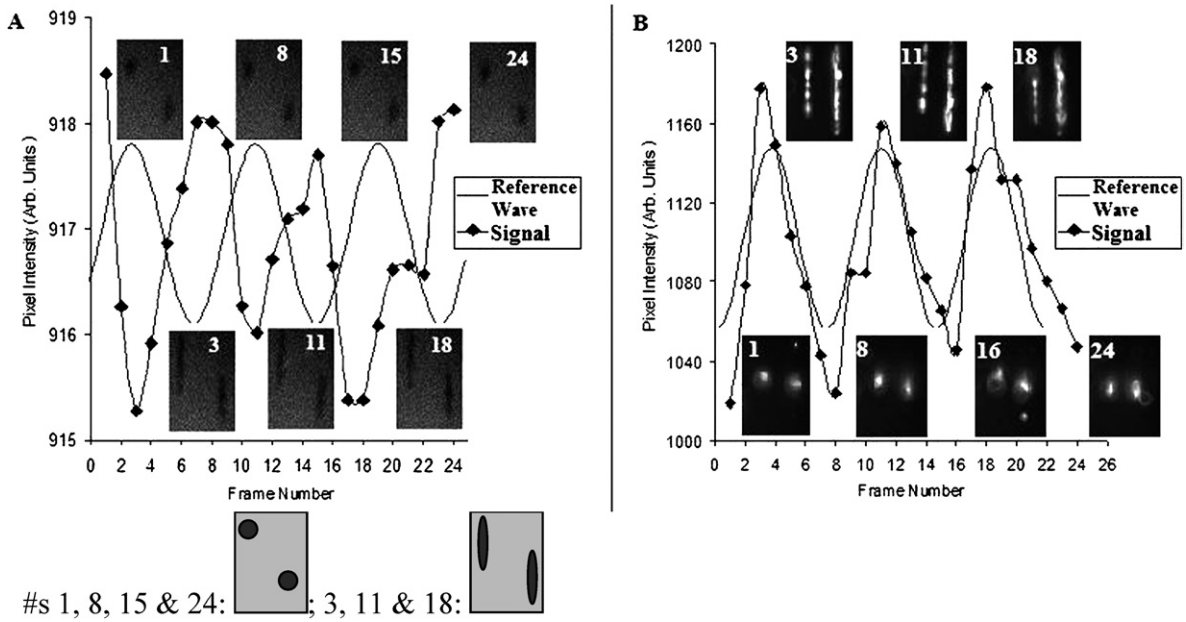

Fig. 1 Example pictures of raw data, average pixel intensity per frame, and reference waveform for modulated competitive immunoassays. Example micrographs shown from the 'peaks' and the 'valleys' of the resulting average pixel intensity. (A) Data from competitive assay (10 nM myoglobin) where supraparticle structures are darker than the surrounding solution, resulting in out-of-phase signal and negative values from lock-in calculations. Below (A), drawings are provided to guide the eye, as the dark-on-darker images are difficult to interpret. When the chains are in full-length view, the raw signal is at a trough, and when the chains are orthogonal to the viewing plane, the raw signal is at a peak. (B) Data from competitive immunoassay and resulting signal showing particle structures brighter than the surrounding solution (2 nM myoglobin). Note that the resulting signal is in-phase with the excitation waveform. This generates a net positive value from the lock-in calculations.

DC signal and higher harmonics of the periodic signal. Also, we can expect to expand the dynamic range *via* parallel small-volume analysis with varying amounts of particles per volume. This work suggests a new method to diagnose AMI and demonstrates two new capabilities in an evolving analytical strategy.

Results and discussion

Modulated sandwich assay for protein: myoglobin

As a demonstration of a modulated structure sandwich assay on a protein, myoglobin was investigated from zero to nanomolar concentrations, with the lowest concentration monitored at 50 pM. These analyses were performed in matrices of buffer and serum and yielded very similar results, generating a linear standard curve for concentrations at 50 pM to 2 nM ($R^2 = 0.999$, Fig. 2A and 2B, Table 1) for buffer and 50 pM to 1 nM ($R^2 = 0.991$, Fig. 2C and 2D, Table 1) for serum. Calculated detection limits were determined from the slope, the signal zero-crossing and two standard deviations of the noise at zero concentration. The experimental detection limits for both were 50 pM (approximately 2 attomole/particle), and the calculated values were 70 pM for buffer and 30 pM for serum. Poorer results were obtained from a static assay of aggregated particles that simulate traditional fluoroimmunoassay strategies (Fig. 3, Table 1). Note that there is a significant difference between modulated sandwich assay, represented by Fig. 2C, and the static sandwich assay, represented by Fig. 3C. The limit of detection for the modulated assay is approximately half that of the static assay. The background (intercept) and sensitivity (slope) are significantly increased for the static assay (1030 *vs.* 17 and 1200 *vs.* 395, respectively). The ratio of the slope to intercept values (one rudimentary method to compare assays) is 20 times higher for the modulated assay. Finally, the linearity is significantly improved for the modulated assay (0.991 *vs.* 0.927).

The assay is performed with a high load of primary and secondary antibodies and high labeling of the secondary antibody (approximately 20 labels per antibody) to drive the assay to the lowest detection limit available with a given set of equilibrium constants. Assuming 40 nmol/mL effective binding sites for the paramagnetic particles (given by manufacturer), the concentration of binding sites in the colloid is 0.4 μM, some hundred to thousand times the antigen concentration. A simple calculation using a simplified $K_{eq} = [Ag–Ab]/[Ag][Ab] = 10^9\ M^{-1}$ ([Ag–Ab] is the bound concentration, [Ag] is the antigen concentration, and [Ab] is the effective antibody concentration) gives an equilibrium value for the 1 nM concentration of myoglobin of [Ag–Ab] = 10^{-7} M, but there is only nanomolar concentration of antigen. A similar argument can be made for the secondary antibody where the equilibrium concentration of antibody–antigen–antibody is calculated to be approximately 30 μM. Under these conditions, it is concluded that essentially all of the antigen is binding to the antibodies, and the signal is effectively linear with concentration over these ranges. For larger ranges, other forms of binding equations will be needed. However, one strategy that can be employed with the small-volume assay is parallel analyses focused and designed for specific linear ranges. This strategy

View Online

Published on 16 December 2008 on http://pubs.rsc.org | doi:10.1039/B809665A
Downloaded by Arizona State University on 06 November 2010

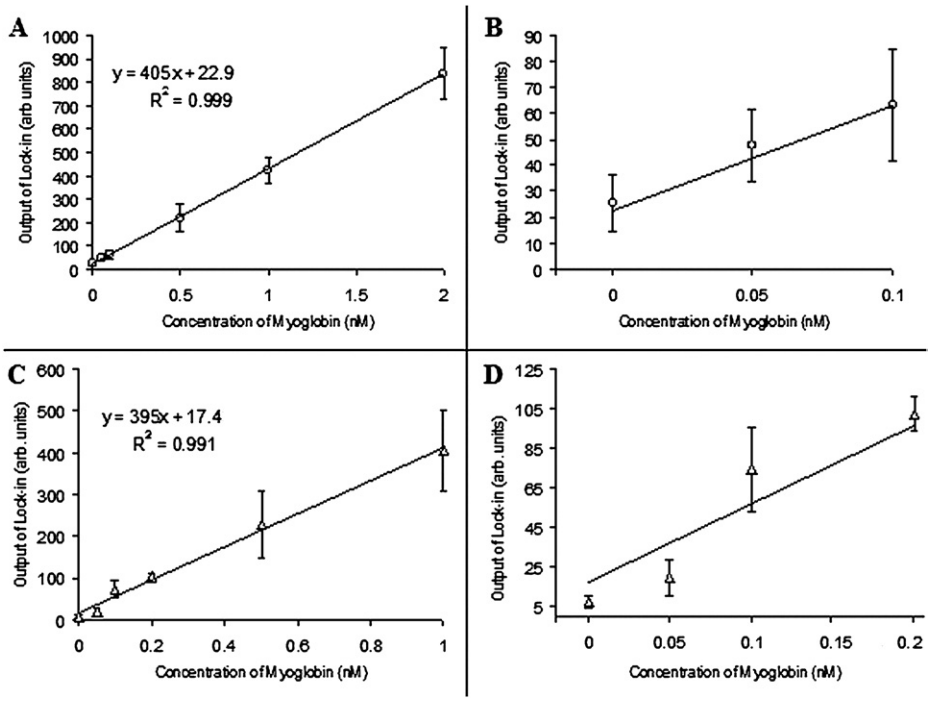

Fig. 2 Standard curves generated from modulated sandwich fluoroimmunoassays in buffer (A, B) and serum (C, D). The modulated sandwich assay has good sensitivity and can accurately quantify the amount of myoglobin in a serum sample. (A) Standard curve generated from the modulated sandwich assay performed in buffer. (B) Expanded view of the lower concentration range from the modulated sandwich assay performed in buffer. (C) Standard curve generated from the modulated sandwich assay performed in serum. (D) Expanded view of the lower concentration range, from the modulated sandwich assay performed in serum media.

Table 1 Numerical comparison of figures of merit for various immunoassays

	Experimental LOD (calculated value[a])	Sensitivity (arb. units/nM)	Intercept (arb. units)	Dynamic range (10^x)	R^2
Buffer					
Sandwich					
Static	500 pM (250 pM)	768	+1080	0.6	0.983
Modulated	50 pM (70 pM)	405	+23	1.6	0.999
Competitive					
Static	N/a	—	—	—	—
Modulated	2.5 nM (3.5 nM)	−2.2	+15	0.3	—
Serum					
Sandwich					
Static	100 pM (96 pM)	1200	+1030	1.0	0.927
Modulated	50 pM (30 pM)	395	+17	1.3	0.991
Competitive					
Static	N/a	—	—	—	—
Modulated	2.5 nM (3.3 nM)	−1.6	+7.3	0.3	—

[a] The calculated LOD is two times the standard deviation at zero concentration times the slope.

would allow for continued use of this rather simplistic approach to quantification.

Modulated competitive myoglobin assay

For this competitive assay, as expected, higher concentrations of unlabeled myoglobin caused the average lock-in output to decrease over the range from 1 to 10 nM (Fig. 4). Background matrix changes from buffer to serum gave a generally similar response, differing only in slope and saturation value. Static aggregate assays in the competitive mode failed to generate any interpretable results in the concentration range studied (Fig. 5).

One complicating factor that differentiates the buffer and serum matrix experiments is the background fluorescence from the bulk solution. This particular problem is unique to the competitive assay strategy. When higher concentrations of unlabeled myoglobin were introduced, more of the fluorescently-labeled myoglobin was observed in the background solution.

 This journal is © The Royal Society of Chemistry 2009

View Online

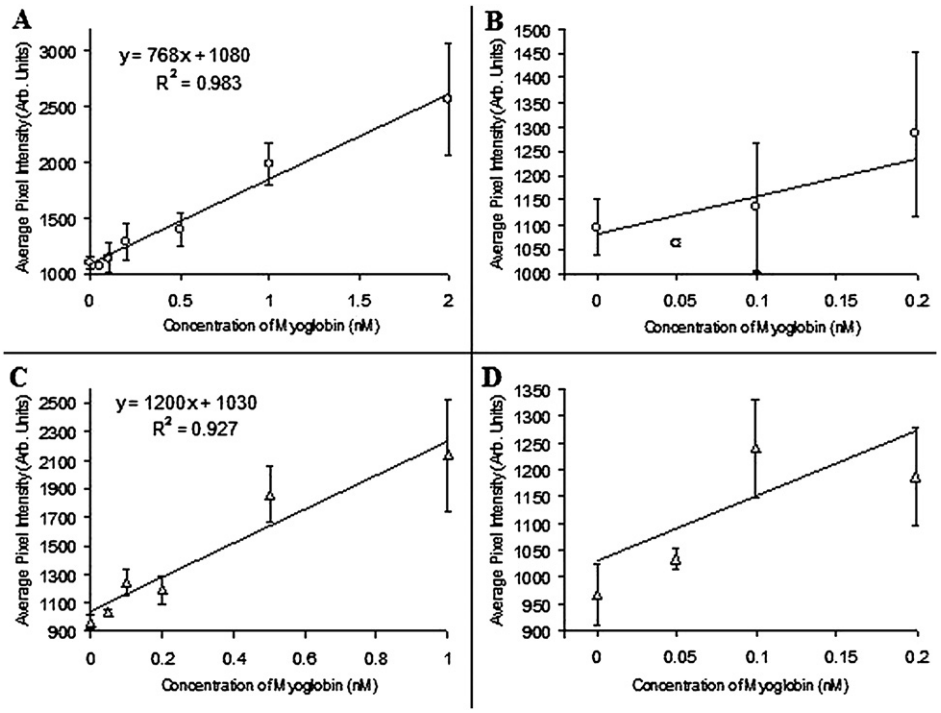

Fig. 3 Standard curves generated from the static aggregate sandwich assay performed in buffer (A, B) and serum (C, D). Without particle modulation the sandwich assay loses accuracy, range, and sensitivity in the quantification of myoglobin. (A) Standard curve generated from the aggregate sandwich assay performed in buffer. (B) Expanded view of the lower concentration range from the aggregate sandwich assay performed in buffer. (C) Standard curve generated from the aggregate sandwich assay performed in serum. (D) Expanded view of the lower concentration range for the aggregate sandwich assay performed in serum.

Published on 16 December 2008 on http://pubs.rsc.org | doi:10.1039/B809665A
Downloaded by Arizona State University on 06 November 2010

Background fluorescence obscures the image, preventing observation of the relatively non-fluorescent rotating structures bound with high concentrations of unlabeled myoglobin. This leads to a noisy raw signal, which still yields a (small) positive value when lock-in calculations are performed. However, when analyzing data from the competitive serum assay, a wash step was included to remove most of the unbound labeled myoglobin. This particular issue can be addressed in future experiments by optimizing the antibody and labeled antigen concentrations.

Another unique feature to the signal generated from the competitive assay is that it dips below zero for higher concentrations. At higher analyte concentrations, particles are darker than the surrounding background matrix, generating an apparent out-of-phase signal (Fig. 1). The images are brighter overall when the supraparticle structures are minimally exposed to the imaging system. However, and importantly, this does not preclude the quantifying of data – as a direct result of the lock-in amplification technique. The technique simply provides a negative value for increasing intensity of out-of-phase signal. For static measurements, such a strategy would be impossible. Performing lock-in calculations on average pixel intensities obtained from these images resulted in negative values for concentrations greater than or equal to 5 nM (Fig. 1 and Fig. 4).

Optimizing a competitive immunoassay with this new technique is complex. In this instance, optimization suggests the lowest possible detection limit and largest dynamic range with a given set of equilibrium constants for the antibody–antigen and the antibody–labeled-antigen interactions. First, the impact of antibody concentration and the antigen concentration range for homogeneous systems is well studied and appears in textbooks (Wild, 2005).[30] In this system it is a bit more complicated because the interaction is a particle–surface interaction, but the capture takes place in bulk solution while the detection occurs at a surface. Additionally, there are potentially overlapping diffusion depletion zones across the bulk buffer. The experiment is performed in a hybrid manner. Using the homogeneous model is instructive, but the bulk concentration is defined by the size and number of paramagnetic particles and the binding-site density. In turn, the size and number of particles can influence the supraparticle structure formation and dynamics. In addition, capture and formation of supraparticle structures, modulation strategies (magnetic field strength and frequency or complex waveform), and signal capture and processing (or image analysis) can all dramatically impact the performance of the technique. Capture and formation strategies have been discussed elsewhere, in some depth,[31,33,34,36–44] whereas frequency or complex waveform strategies for modulation have not been addressed yet.

Fully exploiting modulated immunoassays

Signal capture and image processing are being investigated in a new study[35] indicating that greatly improved detection limits can be generated by identifying and reducing background elements and reducing the variation in the signal intensity at the lower concentrations for the sandwich assay strategy. To begin to discuss the relative success of the lock-in strategy and the potential for improved detection limits and dynamic range, a brief discussion of the source of noise and signal is warranted.

View Online

Published on 16 December 2008 on http://pubs.rsc.org | doi:10.1039/B809665A
Downloaded by Arizona State University on 06 November 2010

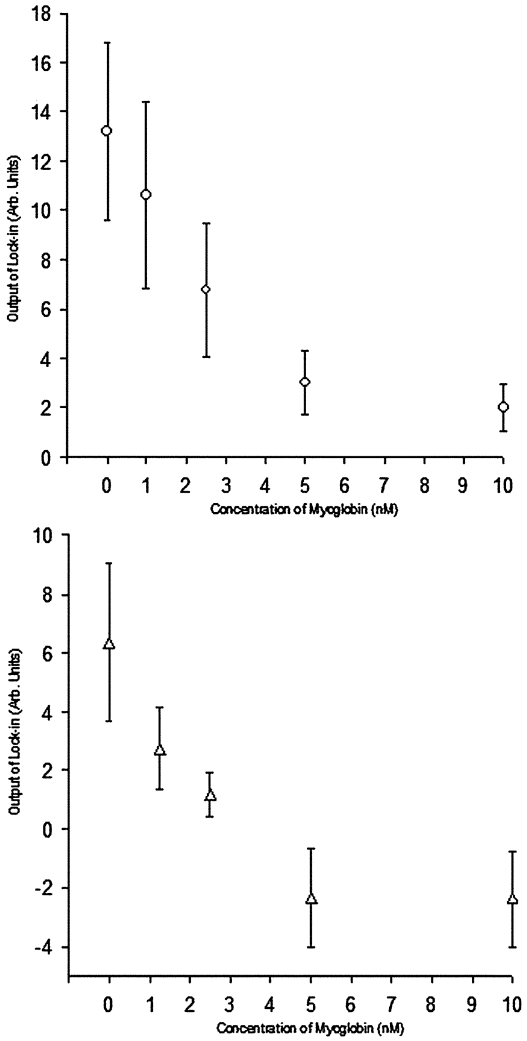

Fig. 4 Standard curves from the modulated competitive assay performed in buffer (top, ○) and serum (bottom, △). Error bars are the standard deviations of the average lock-in output from all droplets analyzed for a given concentration. The serum data were obtained after a wash step, whereas the buffer data were obtained directly after incubation sandwich assay performed in serum.

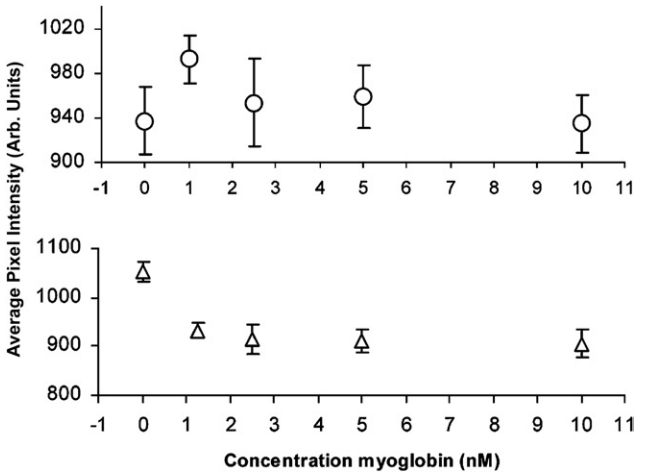

Fig. 5 Standard curves generated from the competitive static aggregate assay performed in buffer (top, ○) and serum (bottom, △). Error bars represent the standard deviations for average pixel intensities obtained from different droplets. The serum data were obtained after a wash step, whereas the buffer data were obtained directly after incubation.

Not using any filtering or signal processes – a classic static assay – greatly limits the ability to discern background and noise from signal associated from the binding event (Fig. 3 and Fig. 5 and previous work[31]).

Most noise is contained in the lower frequency ranges, or DC measurements. By encoding some of the signal power at the frequency and phase of the rotation of the particle structures and monitoring only that range, the signal significantly decreased, but by much less than the noise. This results in a lower intensity signal and a much improved signal-to-noise ratio, thus describing the modest success of the lock-in strategy. However, the lock-in approach is far from optimal and does not effectively capture all of the power available in the encoded signal. For instance, the actual waveform that results from observing the rotors is a rectified sine wave (or similar waveform) at approximately twice the rotating magnetic field frequency, in addition to a significant signal within the DC portion (primarily from the center portion of the rotors). The lock-in strategy only captures a small fraction, or a few percent, of this intensity.

Further, our image analysis includes the entire captured image, not just the rotors. A dramatic improvement can be gained simply by identifying the pixels that contain rotors for inclusion in the data. Another subtlety that will dramatically impact the competitive assay detection is the variation of signal intensity across the image. Our present system created differing signals from the same rotors at differing locations, suggesting that the system is either not evenly illuminated or the capture optics are not optimized. This results in both a larger variation in the background and the signal. Both of these variations negatively impact the detection limit and standard deviation of the signal, which strongly impacts the competitive assay mode. This uneven illumination can be minimized, but not eliminated, with better optics and light source. In addition, the effects on the final results can be minimized through computation.

It should be noted that the dynamic range of the assay can be extended on the high concentration side by increasing the number of particles for the sandwich assay or reducing the sample volume through dilution. This is a feasible mechanism for dynamic range extension since the sample volume can be extremely small and several analyses can be executed in parallel. There are more complicating issues with the competitive approach, but similar strategies can be employed.

We are justifying this work with a longer term goal of developing a method for use in an ambulance or in the emergency room that would allow for faster patient diagnosis and treatment creating a better chance of AMI survival. The current assay would need to be much more fully developed and engineered. The important issues in terms of time, complexity and data analysis can be reasonably addressed. Existing microfluidic strategies can be used that exploit the enhanced mass transport of the colloidal particles and the efficiency of sequestration for wash step and discrete manipulation. Future efforts would include using automated analysis using existing technologies achieved

 This journal is © The Royal Society of Chemistry 2009

View Online

through software development or the adaptation of an avalanche photodiode detector (APD). Analysis with an APD would allow the generated signal to be fed directly into a lock-in amplifier device resulting in instantaneous readings. An APD could also be coupled with LED light sources and fiber optics to achieve device miniaturization. Further work in supraparticle structure containment would allow a greater reduction of the amount of serum needed per analysis and would allow for minimization of error in measurements due to better control over supraparticle structure size and numbers. The present experiments imaged 15 μL droplets containing large populations of paramagnetic structures, but an average of only two structures was analyzed. Isolation and containment of these two structures would greatly reduce the volume of serum needed. Existing flow-cell technologies have shown that containment and rotation of these structures is possible using a cell with a chamber volume of 5.3 nL.[38] Further development and incorporation of all of these technologies into a device would allow rapid analysis of serum samples leading to quicker AMI diagnosis.

Published on 16 December 2008 on http://pubs.rsc.org | doi:10.1039/B809665A
Downloaded by Arizona State University on 06 November 2010

Experimental

Protein conjugation to fluorescein-5-EX, succinimidyl ester

Two milligrams of lyophilized cardiac equine myoglobin (MW ≈ 16 950, Sigma, St. Louis, MO) was dissolved into a 1.5 mL-volume centrifuge tube containing 1 mL of 100 mM carbonate buffer, free of sodium azide at a pH of 8.5. One milligram of fluorescein-5-EX, succinimidyl ester (FEXS, Invitrogen, Carlsbad, California) was dissolved into a 0.5 mL-volume centrifuge tube containing 0.1 mL of DMSO (Sigma, St. Louis, MO). The FEXS solution was immediately added dropwise to the myoglobin solution at room temperature. This was allowed to react for an hour in darkness at room temperature on a Vortex Genie-2 (VWR Scientific, West Chester, PA). The crude reaction mixture was placed into a dialysis membrane with a cut-off value of 1 kD (Sigma, St. Louis, MO). The mixture was dialyzed against 5 exchanges of 1 L of 100 mM phosphate buffered saline (PBS) at a pH of 7.4 with 0.1% sodium azide (Sigma, St. Louis, MO). The solution outside of the membrane was monitored spectroscopically for fluorescence to ensure that dialysis had gone to completion.

A 1 mL aliquot of polyclonal goat anti-equine myoglobin (Pab, Immunology Consultants Laboratory, Inc., Newberg, OR), 1 mg/mL, was initially dialyzed to remove existing sodium azide preservative. The Pab was then reacted in the same manner as cardiac equine myoglobin.

Quantifying the degree of protein conjugation

Dialyzed FEXS-myoglobin and FEXS-Pab were analyzed by absorbance measurements (U-2000 spectrophotometer, Hitachi, Tokyo, Japan). From these measurements, it was determined that 1–2 FEXS molecules were conjugated to a single myoglobin molecule and ~20 FEXS molecules were conjugated to a single Pab molecule. It is noted that a lower degree of labeling on the Pab could be accomplished in the future by dialysis followed by exchange or desalting column. The proteins were then stored at 4 °C until used.

Preparation of primary antibody and particles

BioMag paramagnetic particles, average diameter of 1.6 μm with streptavidin functionalized on their surface (Qiagen, Inc., Valencia, CA) were used to form the supraparticle structures. Biotinylated-anti-equine myoglobin polyclonal antibodies (B-Pab, Immunology Consultants Laboratory, Inc., Newberg, OR) were stored at 4 °C in PBS buffer with sodium azide. Three microliters of paramagnetic particle stock solution was added to 100 μL of B-Pab (1 mg/1 mL) and diluted to a final volume of 300 μL using 100 mM PBS at a pH of 7.4 with 0.1% sodium azide and 5% bovine serum albumin (BSA). This mixture was allowed to react for 3 hours on a Vortex Genie-2. The particles were then washed five times and stored in PBS buffer with sodium azide at 4 °C.

Competitive myoglobin assay (preparation of buffer solutions)

Assay solutions were made using 30 μL of the B-Pab-particle colloid combined with 15 μL of 20 nM FEXS-myoglobin and 15 μL of unlabeled cardiac myoglobin concentrations. The final concentration of FEXS-myoglobin was 5 nM for every unlabeled myoglobin concentration analyzed. These buffer solutions were incubated for 1 hour on a Vortex Genie-2 and were not washed prior to analysis. Readings (15 μL droplets) were taken on an inverted microscope using the modulated assay method along with a static aggregate method.[31]

Competitive myoglobin assay (preparation of serum solutions)

Experiments were repeated using adult bovine serum (MP Biomedicals, Aurora, OH), containing a total protein concentration of 7.24 g/dL. Serum samples were doped with various concentrations of unlabeled cardiac equine myoglobin and 5 nM FEXS-myoglobin. All dilutions used strictly serum so that the samples were in 100% bovine serum. The volumes of buffer in the B-Pab-paramagnetic particle solutions were replaced with doped 60 μL serum samples. Each individual sample was allowed to incubate on a Vortex Genie-2 for only 10 minutes. Due to the higher viscosity of serum, the ability of the paramagnetic particles to rotate was affected. However, this issue was resolved by replacing the serum volume with a wash of PBS buffer after the 10 min incubation. Samples were analyzed immediately.

Sandwich myoglobin assay (preparation of buffer solutions)

Assay solutions were made using 30 μL of the B-Pab-particle colloid combined with 30 μL of unlabeled cardiac myoglobin concentrations. These buffer solutions were then incubated for 1 hour on a Vortex Genie-2. FEXS-Pab stock ssolution (1 μL) was added to each solution and allowed to incubate for an additional hour on the Vortex Genie-2 followed by 10 washes with PBS buffer.

Sandwich myoglobin assay (preparation of serum solutions)

For serum analysis, 30 μL of buffer from the B-Pab-particle solution was replaced with 60 μL of serum doped with varying amounts of cardiac myoglobin. These solutions were incubated for 1 hour on a Vortex Genie-2 and washed once with PBS buffer. FEXS-Pab stock solution (1 μL) was added to each

View Online

Published on 16 December 2008 on http://pubs.rsc.org | doi:10.1039/B809665A
Downloaded by Arizona State University on 06 November 2010

solution and allowed to incubate for an additional hour on the Vortex Genie-2. The particles were washed 10 times with PBS buffer and analyzed on an inverted microscope in the same manner as the competitive assay.

Data collection for modulated structures and aggregate assays

Data were collected on an Olympus I × 70 inverted microscope (Tokyo, Japan) with a charge coupled device (CCD) camera connected to a computer with image-capture capability (QICAM Fast 1394, QImaging, Burnaby, Canada) as previously described.[31] Multiple 15 μL-sized droplets were analyzed for each assay solution using a microscope slide with a concavity (LabScientific, Livingston, NJ). A cylindrical rare earth magnet (2.75 cm diameter, 0.25 cm thick) was used to generate the magnetic field (EdmundScientific, NY). The magnet was mounted to a 7 cm-long rod connected to a DC motor controlled *via* a custom-designed circuit. For the modulated structure assay, the magnet was rotated at a constant frequency, typically at 1.5 Hz. For the aggregate assay, the magnet was used to collect the particles into an aggregate and was not rotated. In both assays, illumination from a mercury lamp was passed through the appropriate filter cube and a 40× objective to excite the assay solution. Emitted fluorescence was then collected with the CCD and stored as video.

Data analysis

Video was analyzed using Image J (National Institute of Health, Bethesda, Maryland). The images (348 × 260 pixels) were captured at an exposure time of ~50 ms (gain, 2000; offset, 2600) which translates to a rate of ~20 frames/s. Even though each image displayed many supraparticle structures, the average pixel intensity was measured for selections that included an average of 2 supraparticle structures. The average pixel dimensions of these structures (15 × 90) were determined with measurements on Image J. A box with pixel dimensions of 150 × 120 was used to select these structures (Fig. 1). Each selection in the video segment was analyzed for over 100 consecutive frames. Raw video from the aggregate assays were collected using the same 150 × 120 selection, but the average aggregate size was greater than half the area of the 150 × 120 box. For the modulated assays, the average pixel intensities calculated for each selection were then plotted *versus* time and lock-in amplification calculations were performed on the normalized periodic raw signal as previously described.[31] For the aggregate assay, the average pixel intensity was calculated from the analysis of selected video in over 100 consecutive frames.

Conclusions

Modulated supraparticle immunoassays have been extended to sandwich and competitive modes targeting protein. The performance of a modulated paramagnetic structure competitive assay has demonstrated that serum myoglobin concentrations greater than or equal to 5 nM, indicating AMI-like conditions, can be diagnosed with only a 10 minute incubation time. This assay, combined with the capability of the sandwich assay to accurately quantify serum myoglobin concentrations from 50 pM to 1 nM, could be incorporated into a device for emergency room diagnosis of AMI. Time optimization of the sandwich assay will make it a viable method to rapidly monitor patients' serum myoglobin concentrations. This will lead to a more accurate diagnosis for individuals who have scored a false negative on initial testing. These new assays can lead to an alternate diagnostic technique for AMI patients requiring less than a droplet (15 μL) of blood for analysis.

Acknowledgements

We would like to thank the Graduate and Professional Student Association of Arizona State University for funding of this project. Support from Arizona Applied Nanosensors is greatly appreciated. We would also like to thank Dr Sergi Aksyonov for his assistance in using the Image J program for video analysis. Michelle Meighan is thanked for her editing of the manuscript while in revision.

References

1 D. Nedelkov, U. A. Kiernan, E. E. Niederkofler, K. A. Tubbs and R. W. Nelson, *Proceedings Of The National Academy Of Sciences Of The United States Of America*, 2005, **102**, 10852–10857.
2 D. Nedelkov, U. A. Kiernan, E. E. Niederkofler, K. A. Tubbs and R. W. Nelson, *Molecular & Cellular Proteomics*, 2006, **5**, 1811–1818.
3 National Heart Attack Program Coordinating Committee, S.M. t. T.W.G., *Annals of Emergency Medicine*, 1994, **23**, 311–329.
4 S. Johnston, R. Brightwell and M. Ziman, *Emergency Medicine Journal*, 2006, **23**, 331–334.
5 H. S. Lee, S. J. Cross, P. Garthwaite, A. Dickie, I. Ross, S. Walton and K. Jennings, *British Heart Journal*, 1994, **71**, 311–315.
6 M. Kemp, J. Donovan, H. Higham and J. Hooper, *British Journal Of Anaesthesia*, 2004, **93**, 63–73.
7 A. H. B. Wu, F. S. Apple, W. B. Gibler, R. L. Jesse, M. M. Warshaw and R. Valdes, *Clinical Chemistry*, 1999, **45**, 1104–1121.
8 R. J. Dewinter, R. W. Koster, A. Sturk and G. T. Sanders, *Circulation*, 1995, **92**, 3401–3407.
9 R. J. de Winter, J. G. Lijmer, R. W. Koster, R. J. Hoek and G. T. Sanders, *Annals Of Emergency Medicine*, 2000, **35**, 113–120.
10 C. Montague and T. Kircher, *American Journal Of Clinical Pathology*, 1995, **104**, 472–476.
11 J. Mair, E. Artnerdworzak, P. Lechleitner, B. Morass, J. Smidt, I. Wagner, F. Dienstl and B. Puschendorf, *British Heart Journal*, 1992, **68**, 462–468.
12 D. A. Gornall and S. N. L. Roth, *Clinical Biochemistry*, 1996, **29**, 379–384.
13 E. Matveeva, Z. Gryczynski, I. Gryczynski, J. Malicka and J. R. Lakowicz, *Analytical Chemistry*, 2004, **76**, 6287–6292.
14 E. G. Matveeva, Z. Gryczynski and J. R. Lakowicz, *Journal Of Immunological Methods*, 2005, **302**, 26–35.
15 K. Aslan and C. D. Geddes, *Plasmonics*, 2006, **1**, 53–59.
16 L. Piras and S. Reho, *Sensors And Actuators B-Chemical*, 2005, **111**, 450–454.
17 F. Le Moigne, M. C. Beauvieux, P. Derache and Y. M. Darmon, *Clinical Biochemistry*, 2002, **35**, 255–262.
18 J. P. Laurino, E. W. Bender, N. Kessimian, J. Chang, T. Pelletier and M. Usategui, *Clinical Chemistry*, 1996, **42**, 1454–1459.
19 B. Beneteau-Burnat, B. Baudin and M. Vaubourdolle, *Journal Of Clinical Laboratory Analysis*, 2001, **15**, 314–318.
20 F. S. Apple, R. Ler, A. Y. Chung, M. J. Berger and M. M. Murakami, *Clinical Chemistry*, 2006, **52**, 322–325.
21 F. S. Apple, M. M. Murakami, R. H. Christenson, J. L. Campbell, C. J. Miller, K. G. Hock and M. G. Scott, *Clinical Chemistry*, 2004, **50**, A9–A9.
22 Abbott Point of Care i-STAT Product Info: Cartridge, Cardiact Biomarker Targets, Web page, Schamburg, IL, Accessed: 2008, http://www.abbottpointofcare.com/istat/www/products/cartridges-family.htm.
23 J. F. Masson, L. A. Obando, S. Beaudoin and K. S. Booksh, *Talanta*, 2004, **62**, 865–870.

 This journal is © The Royal Society of Chemistry 2009

View Online

24 M. A. Jimenezclavero, C. Gonzalezrubio, G. Fontan and M. Lopeztrascasa, *Clinical Biochemistry*, 1994, **27**, 169–176.
25 E. Ishikawa, S. Hashida, T. Kohno and K. Hirota, *Clinica Chimica Acta*, 1990, **194**, 51–72.
26 M. Vanblerk, V. Maes, L. Huyghens, M. P. Derde, R. Meert and F. K. Gorus, *Clinical Chemistry*, 1992, **38**, 2380–2386.
27 J. N. Anker, W. P. Hall, O. Lyandres, N. C. Shah, J. Zhao and R. P. Van Duyne, *Nature Materials*, 2008, **7**, 442–453.
28 E. Delamarche, G. Sundarababu, H. Biebuyck, B. Michel, C. Gerber, H. Sigrist, H. Wolf, H. Ringsdorf, N. Xanthopoulos and H. J. Mathieu, *Langmuir*, 1996, **12**, 1997–2006.
29 J. C. Riboh, A. J. Haes, A. D. McFarland, C. R. Yonzon and R. P. Van Duyne, *Journal Of Physical Chemistry B*, 2003, **107**, 1772–1780.
30 D. Wild, ed., *The Immunoassay Book*, Elsevier, Amsterdam, 3rd edn, 2005.
31 M. M. Petkus, M. McLauchlin, A. K. Vuppu, L. Rios, A. A. Garcia and M. A. Hayes, *Analytical Chemistry*, 2006, **78**, 1405–1411.
32 M. A. Hayes, N. A. Polson, A. N. Phayre and A. A. Garcia, *Analytical Chemistry*, 2001, **73**, 5896–5902.
33 M. A. Hayes, N. A. Polson and A. A. Garcia, *Langmuir*, 2001, **17**, 2866–2871.
34 G. M. Hieftje, *Analytical Chemistry*, 1972, **44**, 81A–88A.
35 P. Mahanti, Arizona State University, Tempe, Arizona, masters thesis, 2008.
36 A. Yadav, R. Calhoun, P. E. Phelan, A. K. Vuppu, A. A. Garcia and M. A. Hayes, *IEEE Proceedings – Nanobiotechnology*, 2006, **153**, 145–150.
37 R. Calhoun, A. Yadav, P. E. Phelan, A. Vuppu, A. A. Garcia and M. A. Hayes, *Lab on a Chip*, 2005, **6**, 247–257.
38 A. K. Vuppu, A. A. Garcia, S. K. Saha, P. E. Phelan, M. A. Hayes and R. Calhoun, *Lab on a Chip*, 2004, **4**, 201–208.
39 A. K. Vuppu, A. A. Garcia and M. A. Hayes, *Langmuir*, 2003, **19**, 8646–8653.
40 H. Wang, Y. Zhu, C. Boyd, W. Luo, A. Cebers and R. E. Rosensweig, *Phys. Rev. Lett.*, 1994, **72**, 1929–1932.
41 P. G. deGennes and P. A. Pincus, *Phys. Kondens. Mater.*, 1970, **11**, 189–198.
42 A. T. Skjeltorp, *J. Appl. Phys.*, 1985, **57**, 3285.
43 Y. H. Hwang and X.-l. Wu, *Phys. Rev. E*, 1994, **49**, 3102–3108.
44 J. Liu, E. M. Lawrence, A. Wu, M. L. Ivey, G. A. Flores, K. Javier, J. Bibette and J. Richard, *Phys. Rev. Lett.*, 1995, **74**, 2828–2831.

Published on 16 December 2008 on http://pubs.rsc.org | doi:10.1039/B809665A
Downloaded by Arizona State University on 06 November 2010